*Physical Modelling in Geotechnics – Gaudin & White (Eds)*
*© 2014 Taylor & Francis Group, London, ISBN 978-1-138-00152-7*

# Miniature cone tip resistance on silty sand in centrifuge model tests

J.H. Kim, S.R. Kim, H.Y. Lee, Y.W. Choo & D.S. Kim
*KAIST, Yuseong-Gu, Daejeon, Republic of Korea*

D.J. Kim
*Hyundai Engineering and Construction, Co., Ltd., Seoul, Republic of Korea*

ABSTRACT: Cone penetration tests were performed on silty sand in a centrifuge to investigate the effects of the scale, size of cone, side boundary and penetration rate. Several penetration tests were performed using an in-flight robot which can be remotely controlled such that it is capable of multi penetration tests into the same soil model without stopping the acceleration. The scale effect was analyzed by the modeling-of-models method. The two tip resistance phases of shallow and deep penetrations were observed. The cone size effect was found only at shallow depths of less than the critical depth, and they diminished at deeper penetration. Finally, the cone tip resistances were correlated with the soil parameters obtained from laboratory tests and the developed relationships were compared to empirical relationships proposed previously.

## 1 INTRODUCTION

Inevitable soil disturbance of in-situ soil samples led to development of in-situ testing. The CPT (cone penetration test) is one of the most popular tools for use in investigations of in-situ soil properties because it provides a continuous profile economically, especially in offshore site investigations.

CPT is also widely used in centrifuge model tests to the same extent it is used in field applications. In order to investigate soil properties in a centrifuge test, miniature cones with smaller cone sizes than the standard size are used. However, it is impossible to simulate the exact diameter of a standard cone in a centrifuge test considering the scales law, as reducing the cone size according to the scaling law is difficult due to fabrication limitations and the grain size effect (Bolton et al. 1999, Balachowski, 2007). Thus, different evaluations between in-situ and centrifuge tests can ensue, even when in-situ the soil condition is precisely replicated in the centrifuge model.

This paper aims to investigate the effect of the scale, size of cone, boundary and penetration rate on the miniature cone tip resistance. Three series of centrifuge model tests were performed on silty sand which was sampled from the Saemangeum site on the western coast of Korea; this site is considered to be an area with high potential for the development of an offshore wind farm. Three different miniature cone penetrometers were developed in this research. A Four-Degree-of-Freedom (4-DOF) in-flight robot equipped at KAIST centrifuge was utilized to push the cones into the soil model at several locations in the container without stopping the centrifuge acceleration. The cone tip resistance was correlated with soil parameters obtained from laboratory tests and the developed relationships were compared with previously proposed empirical relationships.

## 2 TEST APPARATUS

### 2.1 *Miniature cone*

Miniature cones with diameters of 7, 10, and 13 mm and with a conical tip angle of 60˚ were developed, as shown in Figure 1. The tip resistance is directly measured by a load-cell developed in this study. The load-cell is mounted behind the cone tips (Fig. 1a). The load-cell is made of four strain

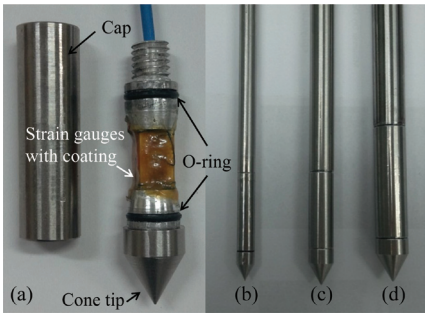


Figure 1. Developed miniature cone penetrometers: (a) load-cell; (b) 7 mm diameter; (c) 10 mm and (d) 13 mm.

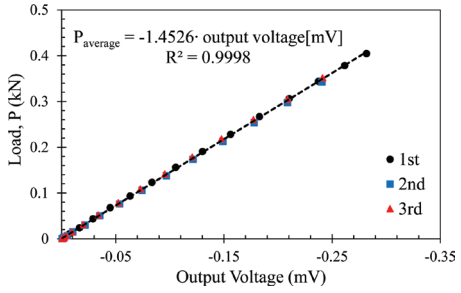


Figure 2. Relationship between the output voltage and the applied load (input voltage = 1V, negative output voltage denotes compression).

gauges connected in a Wheatstone bridge circuit, measuring the load transferred from the cone tip. They were designed with a maximum capacity of 47.5 MPa and a safety factor of 3. The load-cell is covered by hollow cap to prevent interference from the outer soil. The end of the cap is filled with silicone sealant to prevent water from entering the load cell and to prevent the infiltration of soil particles.

### 2.2 *Calibration test*

Calibration tests were conducted to obtain the relationship between the output voltage from the strain gauges and the applied load. The calibration system used for these tests consists of a pedestal and a loading cap. Miniature cones can be fixed on the pedestal and they are covered by the loading cap to transfer the load from the loading equipment. The conical tip was replaced by a ball tip to protect the cone tip. To minimize the friction between the pedestal and the loading cap, grease was spread all over the contact area. An Instron Universal Testing Machine (UTM) was utilized to calibrate the load cell. Continuous loading was applied onto the loading cap at a rate of 0.5 mm/s up to the maximum capacity of the load-cell and the output voltage was simultaneously measured using a SCXI-1314 data acquisition system by NI (National Instruments). The calibration tests were repeated three times and a completely linear relationship between the applied load and the output voltage was obtained, as shown in Figure 2.

## 3 CENTRIFUGE MODELING

### 3.1 *Facilities*

#### 3.1.1 *Geo-centrifuge*

Miniature cone penetration tests in a centrifuge were performed using a beam-type geotechnical centrifuge equipment at KAIST in Korea with a 5 m radius. The maximum capacity of the centrifuge is 240 g tons. The detailed information of the facilities can be found in Kim et al. (2013).

#### 3.1.2 *Four-degree-of-freedom in-flight robot*

A four-DOF robot was utilized to simulate the cone penetration tests in the centrifuge. This on-board robot can be installed on the top of the centrifuge basket and is remotely controlled while spinning the centrifuge. The robot is able to take a tool to any location along three linear directions X, Y, and Z and rotate in one direction, $\theta_z$. Figure 3 shows the 4-DOF robot. The developed miniature cone can be connected to a standard head and then grabbed by the tool holder. Detailed specifications can be found in Kim et al. (2013).

### 3.2 *Penetration tests in silty sand*

To investigate various effects on the cone tip resistance for silty sand in centrifuge models, a series of penetration tests were performed. The tests were conducted with Saemangeum sand sampled from an area near the western coast of Korea. The soil properties of the sand used in this study are given in Table 1.

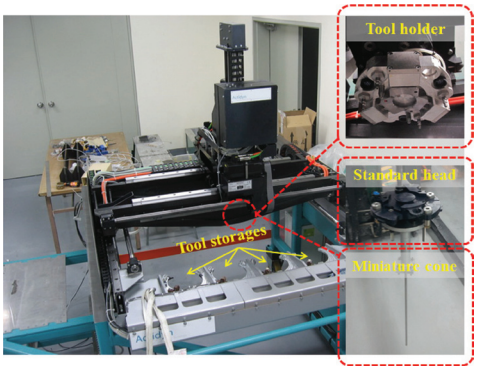


Figure 3. Four-degree-of-freedom in-flight robot.

Table 1. Basic properties of the model soils.

| Items | Properties |
|---|---|
| Specific gravity, $G_s$ | 2.67 |
| Fine contents (passing #200) | 47% |
| Max dry density* (kN/m$^3$) | 16.5 |
| Min. dry density** (kN/m$^3$) | 12.0 |
| Grain size (mm) | $D_{10}$ = 0.045 $D_{50}$ = 0.080 $D_{60}$ = 0.095 |
| Uniformity coefficient, $C_u$ | 2.11 |

*Head (2006). **ASTM 4254 (2002).

Table 2. Conditions of the centrifuge model tests.

| Test no. | $D_r$ (%) | e | $\phi'_p$* (°) | Cone diameter B, (mm) | g-level (g) | Remark** |
|---|---|---|---|---|---|---|
| T1 | 70% | 0.80 | 35.6 | 7 | 71 | M1, M2 |
| | | | | 10 | 50 | M3, M4 |
| | | | | | | BC1~3 |
| | | | | | | PR1~3 |
| | | | | 13 | 38 | M5, M6 |
| T2 | 60% | 0.88 | 33.7 | 10 | 10 | S |
| | | | | | 20 | |
| | | | | | 50 | |
| | | | | | 70 | |
| T3 | 43% | 0.96 | 30.4 | 10 | 10 | S |
| | | | | | 20 | |
| | | | | | 50 | |
| | | | | | 70 | |

*Peak friction angle obtained from a direct shear test. **M = Modeling of models (scale effect), BC = Boundary effect, PR = Penetration rate effect, S = Cone size effect.

The model was prepared by a compaction method to control the target relative density in a cylindrical container. The container dimensions were 700 mm (height) by 900 mm (diameter). In order to prepare a homogeneous soil model, the targeted model height was divided into nine layers. Each layer was compacted to a pre-determined volume and weight using a 13.5 kg circular steel plate from a constant drop height with a constant number of drops, after which static pressure of about 800 kPa was applied. After the preparation of the specimen, water was dribbled from the model surface to saturate the model layers. The prepared model was placed in the basket and the 4-DOF robot with the developed cone was then mounted on the basket. By means of the robot, any position within the container could be reached to perform a penetration test in-flight. After the preparation, the centrifuge spun up to the target g-level of 2 g/min and maintained its targeted acceleration level for 30 minutes to increase the degree of saturation. The cone was penetrated up to 300 mm from the surface at each location with a constant rate of 1 mm/s.

Three series of tests were performed. The tested conditions are tabulated in Table 2. The testing program of this study is illustrated in Figure 4. For T1, the modeling-of-models procedure was applied to investigate the scale effect. Three miniature cones with different diameters were prepared and the penetration tests were performed under different g-levels to simulate a single prototype cone with a diameter of 0.5 m. First, penetration tests were performed using a 13 mm diameter cone at 39 g, after which the centrifuge spinning was stopped. After replacing the cone with the 10 mm cone at 1 g, the centrifuge was accelerated to 50 g and penetration tests were performed. The same process was applied

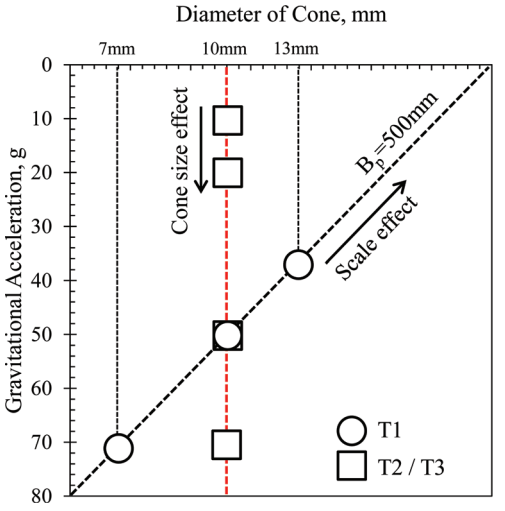


Figure 4. Test program in this study.

for the 7 mm cone at 71 g. Each test therefore modeled a single prototype cone 0.5 m in diameter. The side boundary and penetration rate effects were also studied in T1 to confirm the effects on the tip resistance. These tests were successively performed after the modeling-of-models test using the cone with a diameter of 10 mm at 50 g without stopping the centrifuge spinning. The tested penetration locations are depicted in Figure 5a.

T2 and T3 were used to investigate the cone size effect. Penetration tests using the 10 mm diameter cone were conducted at four elevated g-levels of 10 g, 20 g, 50 g and 70 g, modeled with the 100, 200, 500, and 700 mm diameter cones, respectively.

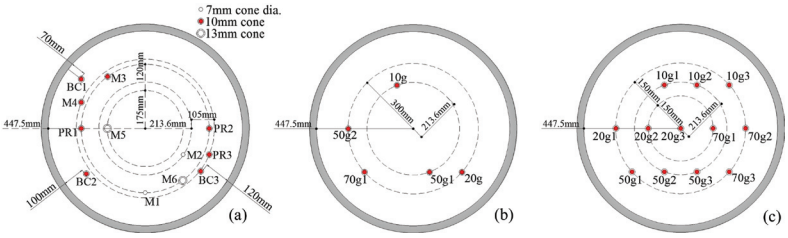


Figure 5. Locations of CPT penetrations in the model: (a) T1; (b) T2; and (c) T3.

All tests were successively conducted at each targeted g-level without stopping the centrifuge spinning. The tested penetration locations are depicted in Figure 5b and 5c.

## 4 TEST RESULTS

Typical profiles of the tip resistance are presented in Figure 6. The tip resistances showed a parabolic increase at a shallow depth and were merged to a certain value at a greater depth, showing a double-curvature profile, as noted by Bolton et al. (1999).

### 4.1 *Modeling of models*

The modeling-of-models procedure was performed in T1 using three cones with different diameters to model a prototype diameter of 500 mm at different g-levels. Figure 7a shows that the three profiles obtained from the cones with diameters of 7-, 10- and 13-mm are mostly superimposed at all depths. This indicates that the cone diameter in the prototype can be modeled properly. This also proves that the soil particle size does not affect the results for a value of $B/D_{50} = 87.5$ because the different ratio of the cone diameter used in this test to the mean particle size shows an identical profile.

### 4.2 *Side boundary and penetration rate effects*

Additional tests were performed to investigate the side boundary and penetration rate effects on the tip resistance. Figure 7b shows the CPTs results conducted at distances of 7B, 10B and 12B from the rigid side boundary. In addition, CPTs were performed with penetration rates of 5, 10 and 20 mm/s. These are compared to the tip resistance results conducted at a penetration distance from the wall to the cone diameter of 15.5B (B; cone dia.) with a 1 mm/sec penetration rate, thus satisfying the recommendations by Bolton et al. (1999). No significant deviations in the tip resistance were found for a boundary condition range of 7B to 15.5B and a penetration rate of 1 to 20 mm/s.

### 4.3 *Cone size effect in cone penetration tests*

The cone size effect was studied under different g-levels using the cone with the 10 mm diameter. Each g-level can simulate a different vertical stress level, modeling different cone diameters of the prototype. The profiles of the cone tip resistance were compared in terms of the prototype, as plotted in Figure 8. At a shallow penetration level, the tip resistance at a given depth of the prototype decreases as the acceleration level increases; this phenomenon markedly appeared in denser sand (T2 > T3). Because no particle size effect was apparent in the modeling-of-models process, this can be attributed to the cone size effect. At deep penetration levels, however, the tip resistance tends to converge regardless of the cone diameter in the prototype.

### 4.4 *Estimation of in-flight soil properties using tip resistances measured at deep penetration levels*

Many researchers have proposed empirical correlations with soil properties from large calibration chamber tests (i.e. Robertson & Campanella 1983, Jamiolkowski et al. 1985). Figure 9 shows the relationship between the bearing capacity number ($q_c/\sigma'_{v0}$) and the peak friction angle as proposed by Robertson & Campanella (1983). Tip resistances under the critical depth in this study were compared with the measured friction angles using direct shear tests. These are included in the graph. For shallow depths, the tip resistance is strongly affected by a low confining pressure and by the cone diameter such that a comparison with previous empirical relationships is difficult. It was noted that the empirical method proposed by Robertson & Campanella (1983) overestimated the friction angle. This overestimation gives the impression that the proposed relationship was only guaranteed for clean moderately compressible quartz sand and not for fine sand in this study.

Figure 10 shows the relationship between the relative density and the cone tip resistance as proposed

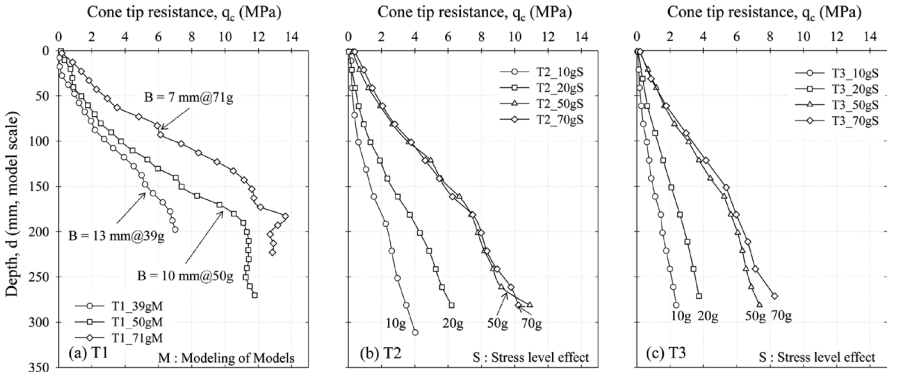


Figure 6. Results of the penetration test for T1, T2 and T3 (in model scale).

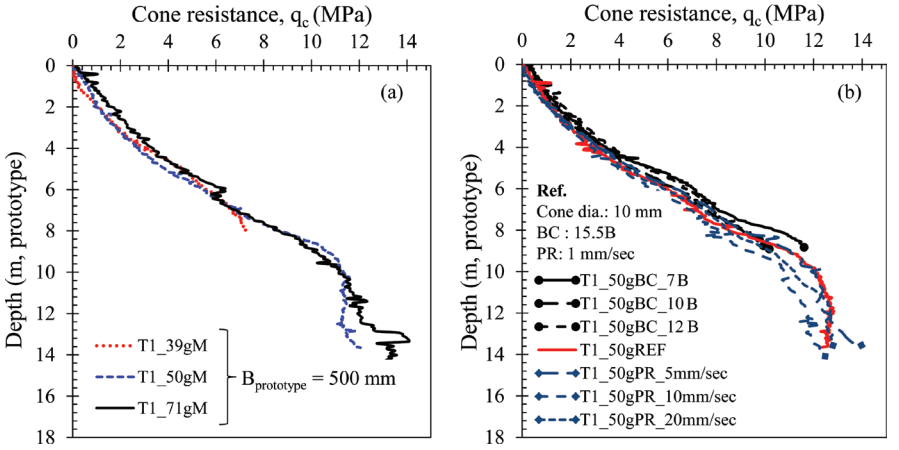


Figure 7. Result of T1: (a) Tip resistances from differently sized cones at different acceleration levels (modeling of models), and (b) effect of the side boundary condition and penetration rate on the tip resistance.

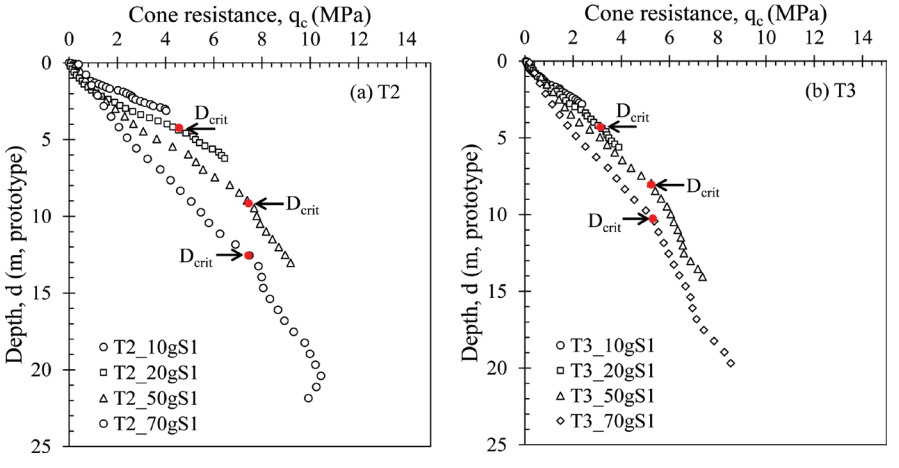


Figure 8. Cone tip resistance with the depth for each g-level (in prototype): (a) T2 ($D_r$ = 60%); (b) T3 ($D_r$ = 43%).

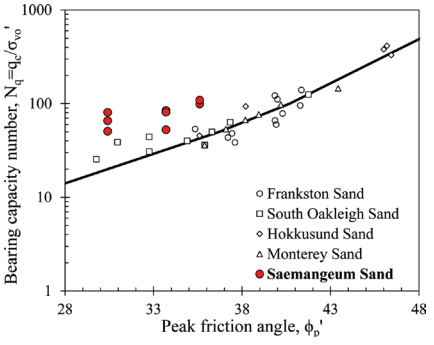


Figure 9. Relationship between the normalized cone resistance and effective peak friction angle and a comparison with the previous result by Robertson & Campanella (1983).

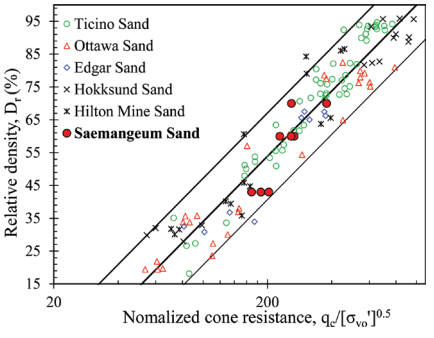


Figure 10. Relationship between the cone tip resistance and relative density ($D_r$) and a comparison with the previous result by Jamiolkowski (1985).

by Jamiolkowski et al. (1985). The tip resistances under the critical depth in this study were added as well. This figure shows that the empirical method estimates the soil properties fairly well.

## 5 CONCLUSION

A series of miniature cone penetration tests were performed in the centrifuge to investigate various effects on the cone tip resistance, in this case the scale, cone size, boundary condition and penetration rate effects. Three miniature cones with different diameter and a calibration system were developed and successfully penetrated into silty sand in a centrifuge using a 4-DOF robot inflight. The modeling-of-models method was used to investigate the scale effect with three cones to model a single-diameter prototype cone at different g-levels. The cone size effect, was studied at different acceleration levels using a cone with a diameter of 10 mm. From the results of this study, the conclusions are as follows:

1. The cone diameter in a prototype can be modeled by the modeling-of-models method; no particle size effect was observed in silty sand with a grain size of $B/d_{50} = 87.5$.
2. The cone size effect with the stress level was observed at a shallow depth but tended to converge after a critical depth. The tip resistance increased with the prototype cone diameter at a given shallow depth and the critical depth increased when increasing the prototype cone size and soil density.
3. No significant boundary or penetration rate effects were observed in a range of 7B to 15.5B and from 1 to 20 mm/s.
4. Friction angles estimated by tip resistances at deep penetration levels using results from Robertson & Campanella (1983) were over-predicted for silty sand. However, the relative densities estimated by the results were well predicted.

## ACKNOWLEDGEMENTS

This study was supported by a grant from the Offshore Wind-energy Foundation System (OWFS) R&D program (10 CTIP E04) of the Korea Institute of Construction & Transportation Technology Evaluation and Planning funded by the Ministry of Land, Transport and Maritime Affairs of Korea and by Hyundai Engineering and Construction, Co., Ltd.

## REFERENCES

American Society for Testing and Materials (ASTM) 2002. *Standard Test Method for Minimum Index Density and Unit Weight of Soils and Calculation of Relative Density.* ASTM D-4254, West Conshohoken, Pa.

Balachowski, L. 2007. Size effect in centrifuge cone penetration tests. *Archives of Hydro-Engineering and Environmental Mechanics* 54(3): 161–181.

Bolton, M.D., Gui, M.W., Garnier, J., Corte, J.F., Bagge, G. & Laue, R. 1999. Centrifuge cone penetration test in sand. *Géotechnique* 49(4): 542–552.

Head, K.H. 2006. *Manual of Soil Laboratory Testing*. London: Whittles Publishing.

Jamiolkowski, M., Ladd, C.C., Germaine, J.T. & Lancellotta, R. 1985. New developments in field and laboratory testing of soils. *Proceeding of the International Conference on Soil Mechanics and Foundation Engineering* 1: 57–154.

Kim, D.S., Kim, N.R., Choo, Y.W. & Cho, G.C. 2013. A Newly Developed State-of-the-Art Geotechnical Centrifuge in Korea. *KSCE Journal of Civil Engineering* 17(1): 77–84.

Robertson P.K. & Campanella, R.G. 1983. Interpretation of cone penetration tests. Part I: Sand. *Canadian Geotechnical Journal* 20: 718–733.